

TURBO: A NOVEL BEAM DELIVERY SYSTEM ENABLING RAPID DEPTH SCANNING FOR CHARGED PARTICLE THERAPY

J. S.L. Yap*, S. L. Sheehy¹, University of Melbourne, Melbourne, Australia
R.B. Appleby², H X.Q. Norman^{2,3}, A. F. Steinberg^{2,3}, University of Manchester, Manchester, UK

¹also at Australian Nuclear Science and Technology Organisation (ANSTO), Australia

²also at Cockcroft Institute, Warrington, UK

³also at University of Melbourne, Melbourne, Australia

Abstract

Charged particle therapy (CPT) is a well-established modality of cancer treatment and is increasing in worldwide presence due to improved accelerator technology and modern techniques. The beam delivery system (BDS) determines the overall timing and beam shaping capabilities, but is restricted by the energy variation speed: energy layer switching time (ELST). Existing treatment beamlines have a $\pm 1\%$ momentum acceptance range, needing time to change the magnetic fields as the beam is delivered in layers at various depths across the tumour volume. Minimising the ELST can enable the delivery of faster, more effective and advanced treatments but requires an improved BDS. A possibility for this could be achieved with a design using Fixed Field Alternating Gradient (FFA) optics, enabling a large energy acceptance to rapidly transport beams of varying energies. A scaled-down, novel system – Technology for Ultra Rapid Beam Operation (TURBO) – is being developed at the University of Melbourne, to explore the potential of rapid depth scanning. Initial simulation studies, beam and field measurements, project plans and clinical considerations are discussed.

INTRODUCTION

The use of charged particle beams as a therapeutic modality has several recognised advantages over conventional treatments as the characteristic ‘Bragg Peak’ enables a precise amount of radiation to be delivered with a greater radiobiological effect. High facility capital costs are prohibitive and new developments in delivery techniques, accelerators and related technologies, along with improved clinical and biological outcomes can better exploit CPT benefits and treatment accessibility. The emergence of methodologies such as ultra-high dose rate ‘FLASH’ [1], Arc [2] and multi-ion [3] therapies also place greater demands on the capabilities of the BDS: significant improvements are needed to overcome existing technical limitations [4].

Although there are many factors which contribute to the delivery process and treatment time, the ELST is a bottleneck constraint and this deadtime whilst waiting for magnetic field adjustments to transport different beam energies has several implications, impacting treatment efficiency and efficacy [5]. As most facilities offer state-of-the-art treatments with active pencil beam scanning, the ELSTs accumulate

and longer beam delivery times translate to higher costs, lower patient throughput and can decrease treatment quality: physical uncertainties and sensitivities with motion cause inferior dosage i.e. ‘interplay effects’ [6]. Numerous mitigation approaches [7] currently used in the clinic to manage uncertainties can be complex to apply and further extend treatment times. Shorter ELSTs, thus faster delivery with the possibility of improved dosimetric quality and robust plans are also particularly beneficial for treating mobile sites [8].

The need for better immobilisation has led to upright treatments being revisited [9] and could offer practical and clinical benefits, notably enabling fixed beamline: gantry-less treatments [10]. This presents the opportunity of not only added cost reduction [11], but in combination with a large energy acceptance BDS with fast ELST, can further improve the effectiveness of standard pencil beam scanning and accommodate new delivery techniques. The applicability for heavier ions could be even greater than for protons given the impracticality of a gantry due to the complexities and infrastructure cost; the increased radiobiological factor may also favour fewer fields and fractions [12]. The clinical advantages and requirements will direct the development of TURBO as a scaled-down, proof-of-concept demonstrator to de-risk these concepts and explore the feasibility of a large energy acceptance BDS for CPT.

TURBO

TURBO comprises several interchangeable modules (A–F as shown in Fig. 1) adapted for the UniMelb low energy ion ‘*Pelletron*’ accelerator [13] (0.5–3.5 MeV protons & He at 100’s nA to several μ A). The FFA section will be curved to accommodate the system requirements for a clinical setting, followed by a fast scanning system downstream to replicate active pencil beam scanning. A self-developed control system will manage all component operation, where precision and synchronicity is required to enable rapid beam delivery.

Initial measurements and beam characterisation studies have been initiated to establish the suitability of the Pelletron for TURBO. Two NEC helical wire beam profile monitors [14] (BPM1,2) and Faraday cups are situated together with the upper and lower slits. These BPMs measure both the horizontal and vertical beam distributions simultaneously but do not give the beam centre position. To determine the beam profile and position, a UniBEaM fibre scanner system [15, 16] was integrated into the beamline ~ 2.10 m downstream of the lower slits. A single motorised (200 μ m diameter) op-

* jacinta.yap@unimelb.edu.au

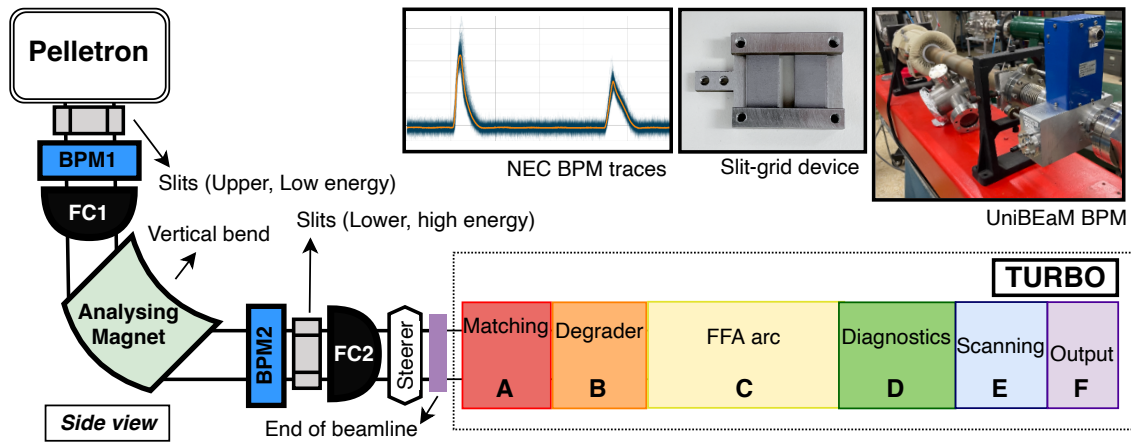


Figure 1: Schematic of the Pelletron and TURBO with key components labelled. Two pairs of vertical and horizontal slits (typically 2.54 mm apart) collimate the beam tails and the vertical bending magnet ensures the desired beam energy. NEC BPM traces, the slit-grid device (with tantalum sheets) and the UniBEaM detector integrated into the beamline are shown.

tical fibre linearly translated across the beam path, provides a signal at each position from detected scintillation light. Three sets of initial measurements were recently obtained with the fibre scanner in the vertical plane (Fig. 2).

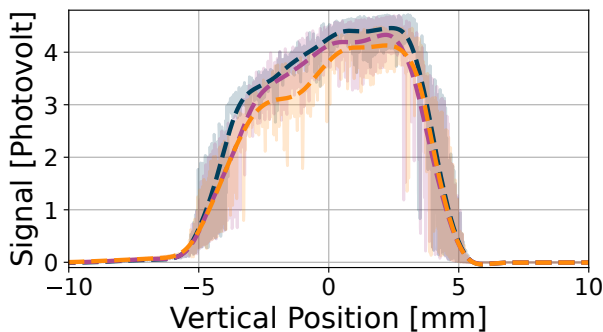


Figure 2: UniBEaM vertical beam profiles. The raw data (shaded), are passed through a low-pass filter to reduce noise.

As full characterisation has not been previously carried out on this machine, slit-grid measurements (Fig. 1) are planned to resolve information about the Pelletron beam phase space and optical parameters [17], and energy measurements using a dipole as a simple spectrometer. Initial modelling suggests a drift of ~ 1 m between the dipole and UniBEaM should produce an energy resolution $<10\%$ at 3.5 MeV. Supplementary imaging diagnostics are also anticipated using (30 & 50 μm thick) YAG screens.

A degrader is necessary to rapidly change the beam energy, requiring a design specific for the low energy range and beam conditions. As protons are easily stopped, varying layers of of different thickness materials were considered; effects of Kapton(R) film were investigated by initial simulations using the Monte Carlo code TOPAS (v3.7.0) [18]. An ideal beam with no angular spread but a uniform distribution over the aperture of the lower slits was generated. A beam of 3.5 MeV (mean) protons can be completely

degraded to 0.1 MeV with 150 μm of Kapton and various energy steps can be attained by combining various standard thickness films: 31 μm generates 3.14 MeV protons; 50 μm , 2.74 MeV; 75 μm , 2.30 MeV; 100 μm , 1.77 MeV; 133 μm , 1.45 MeV and 131 μm , 0.90 MeV. The energy spread grows linearly with increasing Kapton thickness due to multiple coulomb scattering: the beam distribution becomes more Gaussian but the transmission decreases. Subsequent simulations with realistic beam parameters will indicate the need for collimators or additional mitigation to control the spread.

OPTICS

Although ‘FFA optics’ have previously been demonstrated [19], they have never been integrated into an existing accelerator. For TURBO, the beamline is constrained by the beam parameters at either end of the FFA arc: the orbit offsets are not a function of energy at either end, so the optics must constitute a closed-dispersion arc. Also, having zero dispersion at the output makes quality assurance and beam scanning easier. For the input from the Pelletron, we are currently investigating whether a variable matching section is required to ensure that the beam parameters are energy-independent.

Three methods of creating a large energy acceptance arc with zero dispersion at the start and end are discussed in Table 1. One is to use an ‘adiabatic transition’, where the strength of the bending field is smoothly increased over many cells, reaching a maximum at the midpoint of the arc before decreasing symmetrically. Another would be to construct specialised matching cells, to map the input beam optics and offsets to a linear arc by controlling beam trajectories with nonlinear fields and shaped magnet edge angles. The final method is to use nonlinear magnets throughout the arc, setting multipole strengths as are required for stability. Based on the considerations in Table 1, a closed dispersion arc utilising nonlinear optics throughout should provide the most control over the beam dynamics for the full range of energies, while keeping the arc short enough to be viable.

Table 1: Comparison of Methods to Produce a Closed Dispersion FFA Arc

Method	Advantages	Disadvantages
Adiabatic Transition	Uses only linear magnets Simple to design and construct	Smooth transition requires a long beamline Matching is always approximate
Matching Cells	Allows for periodic linear optics in arc Nonlinearity limited to a short region	Errors in matching magnets amplified in arc Dynamics in arc hard to control for all energies
Full Nonlinearity	Fully control dynamics for all energies Tuneable dispersion throughout the arc	Correcting magnet errors over full arc is difficult Aperiodicity requires unique magnets at each point

Fixed field accelerators have been operated using both electromagnets and permanent magnets [19, 20]. For the FFA arc, commercially available permanent magnet blocks are arranged in a plastic 3D printed holder, producing a Halbach array [21] with the desired fields; this is a simplified version of the magnets used for CBETA [22]. An advantage of this method is that it is straightforward to design and construct each unique magnet in the arc rapidly, ensuring that they have the right multipole fields. If an array is no longer required, it is easy to remove and repurpose the magnetic blocks. To verify our plans, a prototype dipole has been modelled, constructed, and measured. Using a maximum of 44 magnetic blocks ($10 \times 5 \times 25 \text{ mm}^3$), the field was compared to modelling in Magpylib [23]. For this prototype (Fig. 3), the internal field was maximised by using 14 sets of 3 magnet blocks in a Halbach cylinder. Although the field quality is poor ($\pm 1.65\%$ in a good field region of $\pm 15 \text{ mm}$ along the midplane), it will be improved with an increased quantity of magnetic blocks in future.

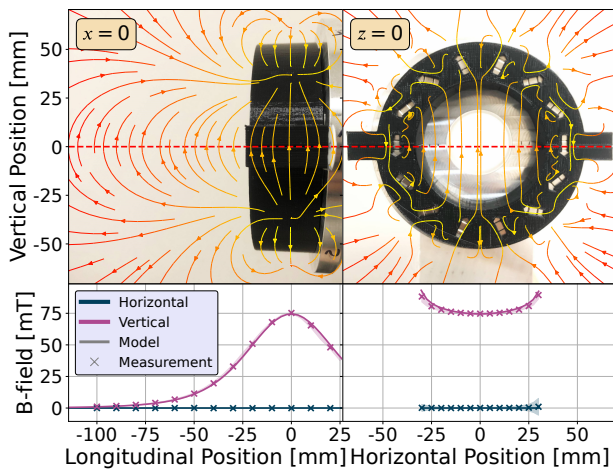


Figure 3: Prototype Halbach dipole with simulated fieldmap. Measurements along the midplane are compared to the predicted field in the lower part of the figure.

TURBO CONCEPT FOR HEAVY IONS

Alongside development of the scaled-down TURBO beamline, work is underway towards a full clinical energy design for transportation of heavier ions. To realise the design, superconducting magnets are required for increased

magnetic fields; Canted Cosine Theta (CCT) is a potential arrangement. The coil geometry produces pure dipole fields whilst cancelling unwanted solenoidal fields [24]; higher order multipoles can be adjusted by modifying the coil windings. Other single-pass optics studies [25, 26] have presented curved, alternating gradient (AG)-CCT configurations, consisting of focusing-defocusing quadrupole layers inside CCT dipoles; [25] reports a momentum acceptance of $\pm 25\%$. Similarly, an AG-CCT arrangement could achieve strong focusing in TURBO to transport a wide range of rigidities without magnet ramping during treatment. Additional clinical specifications being considered for TURBO are described in [4], with magnetic requirements listed in Table 2. The magnetic field ranges are calculated firstly for a bending radius of 2 m. To transport the particles to full treatment energies, three modes are considered. To maintain a similar momentum acceptance from accelerating p^+ to $^{16}\text{O}^{8+}$ requires: $B_{\text{dip}} = (0.62-1.23)\text{T}$ for $E_{p^+, \text{min}}$ to $E_{\text{He}^{2+}, \text{min}}$ ($\frac{\delta P}{P} = \pm 33\%$); $B_{\text{dip}} = (1.25-2.20)\text{T}$ for $E_{\text{He}^{2+}, \text{min}}$ to $E_{\text{C}^{6+}, \text{mid}}$ ($\frac{\delta P}{P} = \pm 33\%$); $B_{\text{dip}} = (2.20-3.65)\text{T}$ for $E_{\text{C}^{6+}, \text{mid}}$ to $E_{\text{O}^{8+}, \text{max}}$ ($\frac{\delta P}{P} = \pm 28\%$). The bore radius of the magnet must also accommodate a suitable treatment field size at patient isocentre (minimum $10 \times 10 \text{ cm}^2$ [27]). The exact design parameters will depend on the optics to determine what higher order multipoles are tolerable. Future modelling of a CCT magnet for TURBO will consider unwanted longitudinal field components in beam dynamics studies [28] and detailed particle tracking through the full 3D field map.

Table 2: Key Clinical Parameters for p^+ to $^{16}\text{O}^{8+}$

Species	E [MeV/u]	$B\rho$ [Tm]	$\pm \frac{\delta P}{P}$	B_{dip} [T]
p^+	70–250	1.23–2.43	33%	0.6–1.22
$^4\text{He}^{2+}$	70–250	2.43–3.32	33%	1.22–1.66
$^{12}\text{C}^{6+}$	70–430	2.50–6.63	45%	1.25–3.32
$^{16}\text{O}^{8+}$	70–500	2.50–7.26	49%	1.25–3.63

The modularity of TURBO allows the flexibility to explore and iterate between different concepts: further experimental, simulation and design work will progress the development of a laboratory implemented demonstrator, to improve beam delivery for existing and future clinical CPT facilities.

REFERENCES

- [1] V. Favaudon *et al.*, “Ultrahigh dose-rate FLASH irradiation increases the differential response between normal and tumor tissue in mice”, *Sci. Transl. Med.*, vol. 6, no. 245, 245ra93–245ra93, 2014, doi:10.1126/scitranslmed.3008973
- [2] X. Ding, X. Li, J. M. Zhang, P. Kabolizadeh, C. Stevens, and D. Yan, “Spot-Scanning Proton Arc (SPARC) Therapy: The First Robust and Delivery-Efficient Spot-Scanning Proton Arc Therapy”, *IJROBP*, vol. 96, no. 5, pp. 1107–1116, 2016, doi:10.1016/j.ijrobp.2016.08.049
- [3] D. K. Ebner, S. J. Frank, T. Inaniwa, S. Yamada, and T. Shirai, “The Emerging Potential of Multi-Ion Radiotherapy”, *Front. Oncol.*, vol. 11, no. February, pp. 1–8, 2021, doi:10.3389/fonc.2021.624786
- [4] J. S. L. Yap, E. R. Higgins, and S. L. Sheehy, “Preliminary Study of a Large Energy Acceptance FFA Beam Delivery System for Particle Therapy”, in *Proc. IPAC’21*, Campinas, Brazil, May 2021, 2021, pp. 1256–1259, doi:10.18429/JACoW-IPAC2021-MOPAB417
- [5] J. Yap, A. D. Franco, and S. Sheehy, “Future developments in charged particle therapy: Improving beam delivery for efficiency and efficacy”, *Front. Oncol.*, vol. 11, 2021, doi:10.3389/fonc.2021.780025
- [6] C. Bert, S. O. Grözinger, and E. Rietzel, “Quantification of interplay effects of scanned particle beams and moving targets”, *Phys. Med. Biol.*, vol. 53, no. 9, pp. 2253–2265, 2008, doi:10.1088/0031-9155/53/9/003
- [7] E. Rietzel and C. Bert, “Respiratory motion management in particle therapy”, *Med Phys.*, vol. 37, no. 2, pp. 449–460, 2010, doi:10.1118/1.3250856
- [8] S. Van De Water, H. M. Kooy, B. J. Heijmen, and M. S. Hoogeman, “Shortening delivery times of intensity modulated proton therapy by reducing proton energy layers during treatment plan optimization”, *Int. J. Radiat. Oncol. Biol. Phys.*, vol. 92, no. 2, pp. 460–468, 2015, doi:10.1016/j.ijrobp.2015.01.031
- [9] S. Rahim, J. Korte, N. Hardcastle, S. Hegarty, T. Kron, and S. Everitt, “Upright Radiation Therapy—A Historical Reflection and Opportunities for Future Applications”, *Front. Oncol.*, vol. 10, no. February, pp. 1–5, 2020, doi:10.3389/fonc.2020.00213
- [10] A. Mazal *et al.*, “Biological and Mechanical Synergies to Deal With Proton Therapy Pitfalls: Minibeams, FLASH, Arcs, and Gantryless Rooms”, *Front. Oncol.*, vol. 10, no. January, pp. 1–14, 2021, doi:10.3389/fonc.2020.613669
- [11] T. R. Bortfeld, M. F. de Viana, and S. Yan, “The societal impact of ion beam therapy”, *Z. Med. Phys.*, pp. 6–8, 2020, doi:10.1016/j.zemedi.2020.06.007
- [12] D. K. Ebner and T. Kamada, “The emerging role of carbon-ion radiotherapy”, *Front. Oncol.*, vol. 6, pp. 6–11, 2016, doi:10.3389/fonc.2016.00140
- [13] R. Colman and G. Legge, “An investigation of the optics of an accelerating column for use with a high brightness ion source and a proton microprobe”, *Nucl. Instrum. Methods. Phys. Res. B*, vol. 73, no. 4, pp. 561–569, 1993, doi:10.1016/0168-583x(93)95840-2
- [14] G. Hortig, “A beam scanner for two dimensional scanning with one rotating wire”, *Nucl. Instrum. Methods*, vol. 30, no. 2, pp. 355–356, 1964, doi:10.1016/0029-554X(64)90299-X
- [15] M. Auger, S. Braccini, T. S. Carzaniga, A. Ereditato, K. P. Nesteruk, and P. Scampoli, “A detector based on silica fibers for ion beam monitoring in a wide current range”, *J. Instrum.*, vol. 11, no. 03, P03027, 2016, doi:10.1088/1748-0221/11/03/P03027
- [16] D. E. Potkins, M. P. Dehnel, T. Kubley, O. F. Toader, and N. R. Lobanov, “UniBEaM - Beam Profiler for Beam Characterization and Position Feedback”, in *Proc. IBIC’17*, Grand Rapids, MI, USA, Aug. 2017, 2017, pp. 335–337, doi:10.18429/JACoW-IBIC2017-WEPCC02
- [17] P. Forck, *Lecture notes on beam instrumentation and diagnostics: Joint University Accelerator School*. 2011.
- [18] J. Perl, J. Shin, J. Schumann, B. Faddegon, and H. Paganetti, “TOPAS: An innovative proton Monte Carlo platform for research and clinical applications”, *Med Phys.*, vol. 39, no. 11, pp. 6818–6837, 2012, doi:10.1118/1.4758060
- [19] S. Machida *et al.*, “Acceleration in the linear non-scaling fixed-field alternating-gradient accelerator emma”, *Nat. Phys.*, vol. 8, no. 3, pp. 243–247, 2012.
- [20] A. Bartnik *et al.*, “Cbeta: First multipass superconducting linear accelerator with energy recovery”, *Phys. Rev. Lett.*, vol. 125, p. 044803, 2020, doi:10.1103/PhysRevLett.125.044803
- [21] K. Halbach, “Design of permanent multipole magnets with oriented rare earth cobalt material”, *Nucl. Instrum. Methods*, vol. 169, no. 1, pp. 1–10, 1980.
- [22] S. J. Brooks, J. Cintorino, A. K. Jain, and G. J. Mahler, “Production of Low Cost, High Field Quality Halbach Magnets”, in *Proc. IPAC’17*, Copenhagen, Denmark, May 2017, 2017, pp. 4118–4120, doi:10.18429/JACoW-IPAC2017-THPIK007
- [23] M. Ortner and L. G. Coliada Bandeira, “Magpylib: A free python package for magnetic field computation”, *SoftwareX*, 2020, doi:10.1016/j.softx.2020.100466
- [24] D. I. Meyer and R. Flask, “A new configuration for a dipole magnet for use in high energy physics applications”, *Nucl. Instrum. Methods*, vol. 80, no. 2, pp. 339–341, 1970, doi:10.1016/0029-554X(70)90784-6
- [25] L. Brouwer *et al.*, “Design and test of a curved superconducting dipole magnet for proton therapy”, *Nucl. Instrum. Methods. Phys. Res. A*, vol. 957, p. 163414, 2020, doi:10.1016/j.nima.2020.163414
- [26] E. Benedetto *et al.*, “A carbon-ion superconducting gantry and a synchrotron based on canted cosine theta magnets”, *arXiv*, 2021, doi:10.48550/ARXIV.2105.04205
- [27] D. S. Robin *et al.*, “Superconducting toroidal combined-function magnet for a compact ion beam cancer therapy gantry”, *Nucl. Instrum. Methods. Phys. Res. A*, vol. 659, no. 1, pp. 484–493, 2011, doi:10.1016/j.nima.2011.08.049
- [28] D. Veres, T. Vaszary, E. Benedetto, and D. Barna, “A New Algorithm for Optimizing the Field Quality of Curved CCT Magnets”, *IEEE Trans. Appl. Supercond.*, vol. 32, no. 5, pp. 1–14, 2022, doi:10.1109/TASC.2022.3162389